NASA Contractor Report 180874
AIAA-88-0714

Consistent Boundary Conditions for Reduced Navier-Stokes (RNS) Scheme Applied to Three-Dimensional Internal Viscous Flows

D.R. Reddy
Sverdrup Technology, Inc.
Lewis Research Center
Cleveland, Ohio

and

S.G. Rubin
University of Cincinnati
Cincinnati, Ohio

January 1988

Prepared for
Lewis Research Center
Under Contract NAS3-24105

National Aeronautics and
Space Administration

ERRATA

NASA Contractor Report 180874
AIAA-88-0474

Consistent Boundary Conditions for Reduced Navier-Stokes (RNS) Scheme Applied to Three-Dimensional Internal Viscous Flows

D.R. Reddy and S.G. Rubin
January 1988

Cover and Report Documentation Page: AIAA-88-0474 should be changed to AIAA-88-0714.

CONSISTENT BOUNDARY CONDITIONS FOR REDUCED NAVIER-STOKES (RNS) SCHEME APPLIED TO THREE-DIMENSIONAL INTERNAL VISCOUS FLOWS

D.R. Reddy
Sverdrup Technology, Inc.
Lewis Research Center
Cleveland, Ohio 44135

S.G. Rubin
University of Cincinnati
Dept. of Aerospace Eng. and Eng. Mechanics
Cincinnati, Ohio 45221

Abstract

A consistent and efficient set of boundary conditions are developed for the multi-sweep space marching pressure-elliptic Reduced Navier-Stokes (RNS) scheme as applied for three-dimensional internal viscous flow problems. No-slip boundary conditions are directly imposed on the solid walls. There is no iteration procedure required in the cross plane to ensure mass conservation across each marching plane. The finite difference equations forming the coefficeint matrix are ordered such that the surface normal velocity is specified on all the solid walls; unlike external flows, a pressure boundary condition in the cross plane is not required. Since continuity is directly satisfied at all points in the flow domain, the first order momentum equations can be solved directly for the pressure without the need for a Poisson pressure correction equation. The procedure developed herein can also be applied with periodic boundary conditions. The analysis is given for general compressible flows. Incompressible flow solutions are obtained, for straight and curved ducts of square cross section, to validate the procedure. The solutions of these test cases are used to demonstrate the applicability of the RNS scheme, with the improved boundary conditions, for internal flows with strong interaction as would be encountered in ducts and turbomachinery geometries.

Introduction

The flow through advanced highly loaded turbomachinery blade rows is characterized by extensive regions of strong three-dimensional viscous-inviscid interaction. To simulate this important pressure interaction, numerical methods that can couple the viscous and inviscid regions must be employed. In addition, efficiency and accuracy of the numerical algorithm become important considerations if these methods are to be useful in the aerodynamic design process.

A number of different approaches have been considered for the simulation of strong viscous-inviscid interaction in internal flows. Conventional full Navier-Stokes (N-S) methods, which solve the full N-S equations throughout the flow field, have been successfully used to analyze three-dimensional interacting flows in turbomachinery blade passages.[1,2] However, these methods do not exploit the asymptotic behavior of the equations at the large Reynolds numbers typically encountered in turbomachinery flows. Consequently, these methods require large computer storage and run times. A recently developed method in this category[1] requires 18 hr of CPU time on a VAX 11/780 computer for the prediction of end-wall flow in a cascade on a relatively coarse grid of 53 by 31 by 10 nodes.

Another approach is interacting boundary layer theory. This has been used by a number of researchers [3-7] for two-dimensional applications, where the interaction of the inviscid flow on the boundary layer is coupled through the injection and surface boundary conditions for the inviscid and boundary layer analysis respectively. These methods are potentially very efficient; however, the evaluation of the injection condition or inviscid displacement body (due to the viscous effects), which alters the inviscid flow, can become rather involved for complex three-dimensional flows. Approximate methods normally used to evaluate this effect, such as linearized small disturbance theory, can result in considerable error. In addition, the approximation of zero normal pressure gradient through the boundary layer might not be appropriate for turbulent flows with strong pressure interaction.[16]

Methods that use space marching with an approximate form of the steady N-S equations (single-pass and multipass marching methods) have been considered for a number of years to predict flows through curved ducts and turbomachinery blade cascades.[8-11] Single pass marching can be used for configurations where the flow is of initial value character, but multiple pass procedures are required for elliptic flows. When applied to elliptic flows, these formulations have generally introduced a Poisson equation for pressure to correct an initially assumed pressure field. This is required in lieu of the continuity equation, which is not satisfied explicitly, in order to ensure global mass conservation. These methods are called partially parabolic or semi-elliptic methods to distinguish them from the full N-S schemes. Although these methods result in less computing time than full N-S methods, the solution of the Poisson equation still requires large computer run times. In addition, due to the uncoupled nature of the pressure correction, which is a necessity of the formulation, extremely large under-relaxation is required in high subsonic and transonic flow regions. This slows down the convergence of the iteration procedure and thereby further increases the run time.

A method that combines the asymptotic treatment of interacting boundary layer theory and the accurate interaction simulation of the full Navier-Stokes methods is the Reduced Navier-Stokes (RNS) formulation. This scheme was originally developed for external flows[12,18] and later formulated for internal flows.[19] The solution procedure and the boundary conditions have been modified in this study to make the scheme more efficient for both two- and three-dimensional flows with strong interaction. As described in earlier references,[14-19] the system of equations resulting in the RNS formulation is similar to that of the partially parabolic scheme in that streamwise diffusion effects are neglected. However, the elliptic effect or upstream influence in strongly interacting flows is simulated by a characteristic treatment of the streamwise pressure gradient. The solution procedure is therefore very much different, and more direct, as compared to that of partially parabolic schemes. The equations are solved by a relaxation procedure with full coupling between pressure and velocities and without the need for a Poisson equation for the pressure correction. Detailed analysis of the RNS scheme and solutions for laminar, turbulent, subsonic, transonic, and supersonic flow regimes for a variety of external flow configurations are given in Refs. 12 to 18. Application of the scheme for internal flow and some preliminary results for two- and three-dimensional internal flows were presented in Ref. 19. As pointed out in these references, the procedure is applicable to both inviscid and viscous flow and can be classified somewhere between interacting boundary layer theory and full Navier-Stokes solvers.

A detailed description and analysis of the RNS scheme as applicable to two-dimensional external flows are given in Refs. 13 to 18. Details of various stages of the evolution of the scheme leading to its present form are also given in Refs. 13, 15 to 17. For the sake of completeness, some of the analysis is repeated here.

The RNS equations were first considered as single sweep or PNS (Parabolized Navier-Stokes) marching procedures for supersonic flows. The first application was for hypersonic flow [20] where the contribution of the streamwise pressure gradient in the corresponding momentum equation is negligible and can therefore be neglected. The equations are mathematically parabolic, upstream influence is negligible, and an exact solution is obtained in a single marching sweep. For lower supersonic mach numbers, where the influence of the streamwise pressure gradient is not negligible, an elliptic effect associated with pressure interaction through the subsonic portion of the boundary layer introduces upstream influence.[21,22] A single sweep methodology then leads to an ill-posed initial value problem and gives rise to exponentially growing departure solutions for a marching step size, $\Delta\xi$, less than $(\Delta\xi)_{min}$ where $(\Delta\xi)_{min}$ is proportional to the extent of the subsonic portion of the flow in the normal (cross stream) direction.[14,23] To surpress this so-called departure effect that reflects the boundary value character of the problem, researchers have used a variety of approximation techniques[20-24] to simulate the elliptic effect of the streamwise pressure gradient term.

In the present RNS procedure, the streamwise pressure gradient term P_ξ is split according to its characteristic behavior so that

$$P_\xi = \omega(P_\xi)_h + (1 - \omega)(P_\xi)_e$$

This follows the eigenvalue analysis of Vigneron et. al,[25] where $0 \leq \omega(M) \leq \omega_{max}$ is a function of local Mach number M and

$$\omega_{max} = \{\gamma M^2/(1+(\gamma - 1)M^2),\ 1\}_{min}$$

As mentioned in Refs. 18 and 19, the portion $\omega(p_\xi)_h$, which is "backward" differenced during discretization, represents the "hyperbolic" or marching part of P_ξ and the term $(1 - \omega)(P_\xi)_e$ represents the "elliptic" or relaxation contribution that is "forward" differenced. Note that for imcompressible flow, since $\omega(0) = 0$, the entire P_ξ contribution iselliptic. "Forward" differencing of $(1 - \omega)(P_\xi)_e$ introduces upstream influence in the computational domain. This removes the ill-posedness found in the single sweep initial value formulation. Due to the forward differencing, the solution procedure requires multiple sweep marching or relaxation. The above treatment of the streamwise pressure gradient, with multiple sweep relaxation, leads to consistent (arbitrary $\Delta\xi$) and departure free ($\Delta\xi \to 0$) solutions for the entire range of incompressible to supersonic Mach numbers. Significantly, only the pressure (and possibly the axial velocity in the limited regions of reversed flow only) need be stored. This results in, among other advantages, a significant reduction in storage requirement over conventional N-S methods.

In the present study, a new consistent solution procedure is formulated, using the RNS Scheme, for three- and two-dimensional flow problems. The treatment of boundary conditions has been significantly modified, compared to the earlier procedure,[19] to make the solution procedure more efficient and accurate. The application of zero injection or solid wall boundary conditions in the cross-plane is more direct in this study than in that of Ref. 19. The procedure is developed for arbitrary compressible flow, but only incompressible solutions are obtained for developing flow in three-dimensional straight and curved ducts of square cross section. These solutions are compared with available experimental data and computed results.

Governing Equations

The governing equations are written in a general curvilinear coordinate system (ξ, η, and ζ) in terms of the primitive variables (u, v, w, p). The momentum equations are then rearranged to reflect the momentum balance in the directions of the contravariant velocity components (U, V, and W). This requires the appropriate combination of the Cartesian component momentum equations after transformation into the ξ, η, and ζ coordinate system. For example, the momentum equation in the U direction is written as ξ_x (x-momentum) + ξ_y(y-momentum) + ξ_z(z-momentum).[26]

The final equations are given in the following matrix form.

Continuity and Momentum:

$$\partial_\xi E + \partial_\eta F + \partial_\zeta G = \partial_\xi R + \partial_\eta S + \partial_\zeta T + K$$

where

$$E = \frac{1}{J}\begin{bmatrix} \rho\zeta U \\ \rho\zeta UU \\ \rho\zeta UV \\ \rho\zeta UW \end{bmatrix}$$

$$F = \frac{1}{J}\begin{bmatrix} \rho\zeta V \\ \rho\zeta VU \\ \rho\zeta VV \\ \rho\zeta VW \end{bmatrix}$$

$$G = \frac{1}{J}\begin{bmatrix} \rho\zeta W \\ \rho\zeta WU \\ \rho\zeta WV \\ \rho\zeta WW \end{bmatrix}$$

$$R = \frac{1}{J}\begin{bmatrix} 0 \\ \xi_x\tau_x{}^{\xi} + \xi_y\tau_y{}^{\xi} + \xi_z\tau_z{}^{\xi} \\ \eta_x\tau_x{}^{\xi} + \eta_y\tau_y{}^{\xi} + \eta_z\tau_z{}^{\xi} \\ z_x\tau_x{}^{\zeta} + \eta_y\tau_y{}^{\zeta} + \eta_z\tau_z{}^{\zeta} \end{bmatrix}$$

$$S = \frac{1}{J}\begin{bmatrix} 0 \\ \xi_x\tau_x{}^{\eta} + \xi_y\tau_y{}^{\eta} + \xi_z\tau_z{}^{\eta} \\ \eta_x\tau_x{}^{\eta} + \eta_y\tau_y{}^{\eta} + \eta_z\tau_z{}^{\eta} \\ \zeta_x\tau_x{}^{\eta} + \zeta_y\tau_y{}^{\eta} + \zeta_z\tau_z{}^{\eta} \end{bmatrix}$$

$$T = \frac{1}{J}\begin{bmatrix} 0 \\ \xi_x\tau_x{}^{\zeta} + \xi_y\tau_y{}^{\zeta} + \xi_z\tau_z{}^{\zeta} \\ \eta_x\tau_x{}^{\zeta} + \eta_y\tau_y{}^{\zeta} + \eta_z\tau_z{}^{\zeta} \\ \xi_x\tau_x{}^{\zeta} + \xi_y\tau_y{}^{\zeta} + \xi_z\tau_z{}^{\zeta} \end{bmatrix}$$

$$K = \frac{1}{J}\begin{bmatrix} 0 \\ \rho\zeta G_{\xi\zeta} - g^{\xi\zeta}p_\xi - g^{\xi\eta}p_\eta - g^{\xi\zeta}p_\zeta \\ \rho\zeta G_{\xi\zeta} - g^{\xi\zeta}p_\xi - g^{\xi\eta}p_\eta - g^{\eta\zeta}\rho_\zeta \\ \rho\zeta G_{\xi\zeta} - g^{\xi\zeta}p_\xi - g^{\zeta\eta}p_\eta - g^{\zeta\zeta}p_\zeta \end{bmatrix}$$

The terms $\tau_x{}^{\xi}$, $\tau_y{}^{\xi}$, etc. appearing in the column vectors R, S, T, and K are explained in detail in Appendix A. The velocities U, V, and W are the contravariant components; all the shear stresses, as shown as Appendix A, can be expressed in terms of these components. Since one of the coordinates (ξ) represents the marching direction, it has been found that the equations in this form enhances the stability of the numerical scheme. In addition, the system of equations in this form can be easily verified for an orthogonal coordinate system. For the sample problems considered in this study, an orthogonal (curvelinear) coordinate system is specified. For the present formulation, adiabatic (wall) conditions are assumed and with a Prandtl number of unity, a simplified energy equation results; i.e., total enthalpy is constant. The same algorithm can also be used for nonadiabatic wall conditions and Prandtl numbers different from unity. The energy equation, written in terms of stagnation enthalpy is only weakly coupled with the remainder of the equations for low speed and even moderate supersonic flows. Therefore, the energy equation can be solved in an uncoupled manner to update the stagnation enthalpy at each marching location. To close the system, an equation of state $p = \rho RT$ and a relation for viscosity, $\mu = \mu(T)$, are required for compressible flows.

In all of the momentum equations, the diffusion terms in the streamwise direction are neglected according to the RNS approximation. These terms are negligible for the coordinate system specified herein so that the RNS system closely approximates the full N-S equations. The flow Reynolds number is based on the inlet uniform velocity and the inlet hydraulic radius of the duct. The pressure is nondimensionalized with the inlet dynamic head.

Discretization

The discretization of the governing equations is illustrated in Figs. 1 and 2. In the marching (ξ) direction the equations are discretized at (i), the velocity node points. In the cross-plane, the continuity, streamwise momentum and the two normal momentum equations are discretized at (c), (ξ), (η), and (ζ), respectively. All of the connective terms in the marching direction are upwind differenced. Both first-order (two point) and second-order (three point) accurate upwind differencing schemes are considered. As discussed earlier, the streamwise pressure gradient, P_ξ is differenced as:

$$P_\xi = (1 - \omega_{i+1})\left\{\left[\frac{P_{i+1}^{n-1} - P_i^{n}}{\xi_{i+1} - \xi_i}\right] + (\Delta p_\xi)_f\right\} + \omega_i\left\{\left[\frac{P_i^{n} - P_{i-1}^{n}}{\xi_i \xi_{i-1}}\right] + (\Delta p_\xi)_b\right\}$$

where the subscript i is a modified index for pressure in the ξ-direction (see Fig. 1) and n is the current marching (global) sweep. The terms $(\Delta p_\xi)_f$ and $(\Delta p_\xi)_b$ are additional correction terms to produce second-order accuracy in the forward and backward directions respectively. These terms are given by:

$$(\Delta p_\xi)_f = \frac{1}{\sigma_f(1 + \sigma_f)(\xi_{i+1} - \xi_i)} \times \left[(1+\sigma_f)\, p_{i+1}^{n-1} - p_{i+2}^{n-1} - \sigma_f p_i^{n}\right]$$

and

$$(\Delta p_\xi)_b = \frac{1}{\sigma_b(1+\sigma_b)(\xi_i - \xi_{i-1})} \times \left[\sigma_b p_i^n - (1+\sigma_b)\, p_{i-1}^n + p_{i-2}^n\right]$$

where

$$\sigma_f = (\xi_{i+1} - \xi_i)/(\xi_i - \xi_{i-1})$$
$$\sigma_b = (\xi_{i-1} - \xi_{i-2})/(\xi_i - \xi_{i-1})$$

For first order accuracy the terms $(\Delta p_\xi)_f$ and $(\Delta p_\xi)_b$ are neglected.

The discretization for p_ξ requires that the unknown pressure p_i at the marching location i, is staggered at a distance $(1-\omega)\Delta\xi$ upstream of velocity u_i, v_i, and w_i. The pressure at the grid point i is given by:

$$\bar{p}_i = \omega_{i+1} p_i + (1 - \omega_{i+1}) p_{i+1}$$

The discretization of all derivatives in the η and ζ cross flow directions is second-order accurate except for one of the viscous terms in each of the normal momentum equations. These terms are the diffusion terms in the same direction as the momentum direction, i.e., the second derivative with respect to η in the η-momentum equation and the corresponding term in ζ momentum equation. Since these viscous terms are negligibly small, i.e., of order of the neglected streamwise diffusion terms, for large Reynolds numbers, the discretization in the η and ζ directions remains essentially second-order accurate. The nonlinear convective terms in the finite difference equations are qualsiliearized, with respect to the previous marching location, using a Newton linearization. The linearized equation result in a coupled system for the vector $[U, V, W, p]^T$. The system of equation can be represented by the matrix equation

$$[A]\ \{\phi\} = \{q\}$$

where $\{\phi\}$ is the solution vector $[U,V,W,p]^T$, $\{q\}$ is the known right hand side of the equation, and $[A]$ is the nine diagonal coefficient matrix shown in Fig. 3. The associated computational molecule is shown in Fig. 4. Each of the elements of the coefficient matrix $[A]$ is a 4 by 4 matrix corresponding to the column size [4] of the vector $\{\phi\}$. The discrete system of equations is solved for $[U,V,W,p]^T_{i,j,k}$ at each marching location i with the modifed strong implicit procedure (MSIP) of Ref. 27. This method was originally developed for the scalar system describing the two-dimensional heat conduction equation.[27] It was modified by the present investigators for application to a vector system of equations in a previous study.[19] The details of the procedure are given in Refs. 19 and 27. As mentioned in Ref. 19 for a two-dimensional flow the cross-plane reduces to a line and the system of equations reduces to a block tridiagonal system for $[U,V,p]_{j,j}$ which is solved by standard LU decomposition.

Boundary Conditions

The method of application of boundary conditions often dictates the efficiency of a solution algorithm. A major change in the RNS/MSIP solution procedure has been implemented in the present study by a modification of the boundary conditions as applied in the previous study.[19]

Inflow and outflow boundary conditions are straight forward. Since streamwise (ξ) diffusion terms are neglected and streamwise convection terms are upwind differenced, the velocities have an initial value character (except in regions of reversed flow). Therefore the velocities must be specified only at the inflow boundary assuming that flow reversal does not occur at the outflow boundary. Due to the splitting of the streamwise pressure gradient into a forward differenced (relaxation) and backward differenced (marching) elements, a pressure condition is required at both the inflow and outflow boundaries for mach numbers $0 < M < 1$. For mach numbers $M \geq 1$, ω becomes unity and therefore a pressure condition is not required at the outflow boundary i.e. full marching. For incompressible flow ($\omega = 0$) a pressure condition is not required at the inflow boundary (full relaxation). For $0 < M < 1$, the staggered pressure (see Fig. 1), leads to a partially prescribed pressure condition at both the inflow and outflow computational planes, since at the node point i,

$$\bar{p}_i = \omega_{i+1} p_i^n + (1 - \omega_{i+1}) p_{i+1}^{n-1}$$

In the cross plane (η - ζ plane), it is important to apply the boundary conditions in a consistent manner if the system of discretized equations is to be solved efficiently. To illustrate the present procedure, let us first consider the two-dimensional flow problem. The cross-plane then reduces to a line, e.g., $0 \leq \eta \leq 1$. The discretization location for the continuity, ξ-momentum and η-momentum, as associated with the node j, are denoted in Fig. 5 by (c), (ξ), and (η) respectively.

As seen in Fig. 5, the number of discrete ξ-momentum equations is $j_{max} - 2$ and the number of descrete η-momentum and continuity equations are each $j_{max} - 1$. Therefore the total number of unknowns is $3j_{max}$ (U, V, and p for each node) and the total number of discrete equation is $(3j_{max} - 4)$. For solid walls ($j = 1$ and $J = j_{max}$), each wall has two physical boundary conditions, i.e., $U = 0$ and $V = 0$. Therefore, the system is closed in so far as total number of equations plus the boundary conditions compared with the number of unknowns is concerned. However, since there are only $j_{max} - 1$ discrete η-momentum equations, the numerical solution procedure apparently requires a condition for pressure at one of the boundaries ($j = 1$ or $j = j_{max}$). This would render one of the boundary conditions on V redundant. In the previous study,[19] the zero normal velocity ($V = 0$) was indirectly imposed at the outer boundary

($j = j_{max}$) through an artificial pressure boundary condition. An iterative process on this pressure boundary condition, imposed at $j = j_{max}$ was required in order to ensure global mass conservation or that the velocity $V = 0$ at $j = j_{max}$. In the present study, the zero injection conditions are directly imposed at both the boundaries without any need for the iterative artificial pressure boundary condition. This is acomplished by slightly changing the structure of the block tridiagonal matrix near the outer boundary. The block tridiagonal system at the marching location (i), for two-dimensional flow, is shown in Fig. 6. For an interior point, $2 \leq j \leq j_{max}-2$, the three equations for the unknown U, V, and p are grouped as:

$$\begin{bmatrix}\text{continuity at } j - 1/2\\ \xi\text{-momentum at } j\\ \eta\text{-momentum at } j + 1/2\end{bmatrix}$$

For the point next to upper boundary (the lower boundary can be chosen instead of upper boundary) we modify the grouping as follows.

$$\begin{bmatrix}\text{continuity at } (j_{max} - 1 - 1/2)\\ \zeta\text{-momentum at } (j_{max} - 1)\\ \text{continuity at } (j_{max} - 1 + 1/2)\end{bmatrix}$$

For wall boundaries (i.e., $j = 1$ and $j = j_{max}$) the structure is given as follows.
For $j = j_{max}$

$$\begin{bmatrix}U = 0\\ V = 0 \text{ (or specified)}\\ \eta\text{-momentum eqn at } (j_{max} - 1+1/2)\end{bmatrix}$$

and for $j = 1$

$$\begin{bmatrix}U = 0\\ V = 0 \text{ (or specified)}\\ \eta\text{-momentum eqn at } (1 + 1/2)\end{bmatrix}$$

The arrangement of the equations and the boundary conditions is shown in Fig. 7.

For periodic boundaries, the surface normal velocities cannot be specified. The total number of discrete equations remains $3j_{max}-4$. However, the number of unknowns is now reduced (Fig. 8), since the values of the unknowns at $j = j_{max}$ are equal to those at $j = 1$.

Therefore the total number of unknowns is now $(3j_{max} - 3)$. This requires only one additional equation to close the system. This condition is obtained by applying the ξ-momentum equation at $j = j_{max}$. This relies on the fact that the location $j = j_{max} + 1$ is equivalent to the location $j = 2$. The resulting periodic block tridiagonal system can once again be solved using the standard LU decomposition.[28]

This procedure can be directly extended to three-dimensinal flows since the η and ζ momentum equations are discretized in exactly the same manner as for two-dimensional flows. The continuity equation is now dicretized at $(j - 1/2, k - 1/2)$ (Fig. 2). Along the lines $j_{max} - 1$ and $k_{max} - 1$, the arrangement of equations is as follows:
For $(j_{max} - 1, k)$

$$\begin{bmatrix}\text{continuity at } (j_{max} - 1/2, k - 1/2)\\ \xi\text{-momentum at } (j_{max} - 1, k)\\ \zeta\text{-momentum at } (j_{max} - 1, k + 1/2)\\ \text{continuity at } (j_{max} - 1-1/2, k-1/2)\end{bmatrix}$$

with a similar form for $(j, k_{max} - 1)$. For interior points, $2 \leq j \leq j_{max} - 1$, the arrangement is given as

$$\begin{bmatrix}\text{continuity at } (j-1/2, k-1/2)\\ \xi\text{-momentum at } (j, k)\\ \eta\text{-momentum at } (j+1//2, k)\\ \zeta\text{-momentum at } (j, k+1/2)\end{bmatrix}$$

The resulting block nine-diagonal matrix system is solved in the same manner with the MSIP scheme. The boundary conditions can be summarized as follows.

Inflow ($\xi = \xi_o$): At the inflow boundary, velocities are specified. A condition on the staggered pressure is required only for the compressible case ($\omega \neq 0$).

Outflow ($\xi = \xi_{max}$): At the ouflow boundary, only one boundary condition on the staggered pressure is required. Either p or $\partial p/\partial \xi$ is specified.

Lower and left wall boundaries ($\eta = 0$, and $\zeta = 0$); No slip and zero injection are specified on the solid walls ($U = 0$, $V = 0$, and $W = 0$). A boundary condition for pressure is not required. The normal momentum equations, at the corresponding boundaries, are applied to obtain the wall pressure (η-momentum equation at $\eta = 0 + \Delta\eta/2$ and ζ momentum equation at $\zeta = 0 + \Delta\zeta/2$).

Upper and right boundaries ($\eta = \eta_{max}$ and $\zeta = \zeta_{max}$): Once again zero injection and no slip are specified on the solid walls. A boundary condition for pressure is not required. The normal momentum equations are applied at the boundaries to obtain the surface pressure (η-momemtum equation at $\eta = \eta_{max} - \Delta\eta/2$ and ζ-momentum equation at $\zeta = \zeta_{max} - \Delta\zeta/2$).

Solution Procedure

Starting from the inflow boundary and then at each marching location i, the block nine diagonal system shown in Fig. 3 is solved with the MSIP algorithm for $[U, V, W, P]^T$. The density and temperature for compressible flows, is updated after the local iteration for the quasi-linearized system has converged at each marching location i. The density and temperature are evaluated using the state and energy equations. The relaxation (marching) procedure proceeds to the downstream boundary. The terms with superscript $(n - 1)$ are then updated from the previous marching sweep or global iteration. The relaxation process from the inflow to the outflow boundaries is repeated until the maximum change in the pressure field for two consecutive global iterations is less than a prescribed tolerance, e.g., 10^{-5}.

Stability

As discussed in Ref. 19, a detailed stability analysis of the relaxation procedure for two-dimensional incompressible flow is presented in Ref. 16 and a similar analysis for compressible flow is given in Ref. 29. The analysis shows that the relaxation procedure for the pressure field is unconditionally stable. Since relation of the pressure field in the marching direction is the same for three- and two-dimensional flows, a similar conclusion can be inferred for three-dimensional flows. For the cross-plane inversion, the MSI procedure has been shown to be unconditionally stable in Ref. 27 Therefore, the overall solution procedure is postulated as unconditionally stable. No stability limitations were encountered in the present calculations.

Results

The three-dimensional flows considered in this study were chosen primarily to validate the scheme and to compare the results with available experimental data and numerical solutions obtained by other schemes. First, a simple case of laminar developing flow in a straight duct of square cross section was considered. As noted previously, the Reynolds number is based on the uniform inlet velocity and the hydraulic diameter H of the cross section. The velocities and lengths are nondimensionalized with respect to the inlet velocity and the hydraulic diameter respectively. The number of grid points used in the streamwise direction is 51 and in the cross plane 11 by 11. The results obtained for incompressible flow were compared with the numerical solution of Rubin and Khosla,[30] obtained using a boundary layer/potential core analysis, and with the experimental data of Goldstein and Kreid[31] (see Figs. 9 and 10). The comparison shows very good agreement of the RNS results with both the earlier numerical results and the experimental data. Next, a slightly more severe case of developing flow in a circular arc (curved) duct of square cross section was considered (Fig. 11). As in the case of the straight duct, the Reynolds number is based on the uniform inlet velocity and the hydraulic diameter of the cross section. The Dean number, which is defined as $Re/\sqrt{R/H}$ is 55, and Reynolds number is 205. Once again, only the incompressible flow solution was obtained, as the data for this case was readily available. The number of streamwise stations was 101, with a grid size of 15 by 15 in the cross plane. The development of the streamwise velocity profiles in the radial plane and in the transverse plane, from the entrance to the fully developed region, is shown in Figs. 12 and 13. The fully developed streamwise velocity profile in the radial plane was compared with the numerical solutions obtained by Kreskovsky et al.,[32] who assumed a parabolic secondary flow correction to the primary flow, Ghia and Sokhey,[9] who used a parabolic method and with the experimental data of Mori et al.[33] The comparison, as seen in Fig. 14, shows good agreement with the numerical results. The experimental data differs from all of the numerical solutions. This disagreement of the experimental results can be attributed to possible inaccuracies in the measurements. Figure 15 shows the comparison of the fully developed secondary velocity profile in the transverse plane with those predicted by Kreskovsky et al.[32] and Ghia and Sokhey.[9] The agreement of the RNS solution with the other numerical solutions is very good. A vector plot of the fully developed secondary velocity in the cross section is given in Fig. 16. This clearly depicts the plane of symmetry and the location of the vorticies that appear away from the axis and toward the outer wall due to the effects of the centrifugal force. Compressible low Mach number solutions were also obtained but are not presented here.

Summary

A consistent procedure has been developed for the application of zero injection and pressure boundary conditions for the RNS algorithm. The matrix structure of the discretized equations has been reordered near the boundaries so the physically meaningful boundary conditions can be applied on the boundaries in a direct manner. Global and local mass conservation is satisfied automatically without the necessity of iteration or a Poisson pressure equation. The modified strongly implicit procedure (MSIP) is used to invert the nine diagonal matrix resulting from the coupled system of equations for velocities and pressure in the cross plane. The procedure has been validated for two example cases, developing flow in straight and curved ducts of square cross section. The solutions are in good agreement with other computed results and experimental data. The scheme will be applied to more complex geometries of practical interest and to compressible flows in future studies.

Acknowledgment

This work was supported under contract No. NAS3-24105 at NASA Lewis Research Center with Dr. Peter Sockol as the project manager.

Appendix A - Transformation

$$\xi = \xi(x,y,z)$$

$$\eta = \eta(x,y,z)$$

$$\zeta = \zeta(x,y,z)$$

The Jacobian J is given by:

$$J = \frac{1}{x_\xi y_\eta z_\zeta + x_\zeta y_\xi z_\eta + x_\eta y_\zeta z_\xi - x_\xi y_\zeta z_\eta - x_\eta y_\xi z_\zeta - x_\zeta y_\eta z_\xi}$$

The contravariant components U, V, and W, written without metric renormalization are given by

$$U = \xi_x u + \xi_y v + \xi_z w$$

$$V = \eta_x u + \eta_y v + \eta_z w$$

$$W = \zeta_x u + \zeta_y v + \zeta_z w$$

where u, v, and w are the Cartesian velocity components in x, y, and z directions respectively. The shear stress terms appearing in the momentum equations are given as follows

$$\tau_x^{\xi} = \xi_x\tau_{xx} + \xi_y\tau_{xy} + \xi_z\tau_{xz}$$

$$\tau_y^{\xi} = \xi_x\tau_{xy} + \xi_y\tau_{yy} + \xi_z\tau_{zz}$$

$$\tau_z^{\xi} = \xi_x\tau_{xz} + \xi_y\tau_{yz} + \xi_z\tau_{xz}$$

$$\tau_x^{\eta} = \eta_x\tau_{xx} + \eta_y\tau_{yx} + \eta_z\tau_{xz}$$

$$\tau_y^{\eta} = \eta_x\tau_{xy} + \eta_y\tau_{yy} + \eta_z\tau_{yz}$$

$$\tau_z^{\eta} = \eta_x\tau_{xz} + \eta_y\tau_{yz} + \eta_z\tau_{zz}$$

$$\tau_x^{\zeta} = \zeta_x\tau_{xx} + \zeta_y\tau_{yx} + \zeta_z\tau_{zx}$$

$$\tau_y^{\zeta} = \zeta_x\tau_{xy} + \zeta_y\tau_{yy} + \zeta_z\tau_{zy}$$

$$\tau_z^{\zeta} = \zeta_x\tau_{xz} + \zeta_y\tau_{yz} + \zeta_z\tau_{zz}$$

where τ_{xx}, τ_{xy}, etc. are the regular Cartesian shear stress components. The Cartesian derivatives are expanded in ξ, η, and ζ space via chain rule relations such as $u_x = \xi_x u_\xi + \eta_x u_\eta + \zeta_x u_\zeta$. The Cartesian velocity components are in turn expressed in terms of the contravariant velocity components defined earlier by the following

$$u = x_\xi U + x_\eta V + x_\zeta W$$

$$v = y_\xi U + y_\eta V + y_\zeta W$$

$$w = z_\xi U + z_\eta V + z_\zeta W$$

Finally, the terms $G_{\xi\zeta}$, $g^{\xi\zeta}$, etc. appearing in the $\hat{K}$ are given as

$$G_{\xi\zeta} = U((\xi_x)_\xi u + (\xi_y)_\xi v + (\xi_z)_\xi w) + V((\xi_x)_\eta u + (\xi_y)_\eta v + (\xi_z)_\eta w) + W((\xi_x)_\zeta u + (\xi_y)_\zeta v + (\xi_z)_\zeta w)$$

$$G_{\eta\zeta} = U((\eta_x)_\xi u + (\eta_y)_\xi v + (\eta_z)_\xi w) + V((\eta_x)_\eta u + (\eta_y)_\eta v = (\eta_z)_\eta w) + W((\eta_x)_\zeta u + (\eta_y)_\zeta v + (\eta_z)_\zeta w)$$

$$G_{\zeta\zeta} = U((\zeta_x)_\xi u + (\zeta_y)_\xi v + (\zeta_z)_\xi w) + V((\zeta_x)_\eta u + (\zeta_y)_\eta v + (\zeta_z)_\eta w) + W((\zeta_x)_\zeta u + (\zeta_y)_\zeta v + (\zeta_z)_\zeta w)$$

$$g^{\xi\xi} = \xi_x^2 + \xi_y^2 + \xi_z^2$$

$$g^{\xi\eta} = \xi_x\eta_x + \xi_y\eta_y + \xi_z\eta_z$$

$$g^{\xi\zeta} = \xi_x\zeta_x + \xi_y\zeta_y + \xi_z\zeta_z$$

$$g^{\eta\varepsilon} = \xi_x\eta_x + \xi_y\eta_y + \xi_z\eta_z$$

$$g^{\eta\eta} = \eta_x^2 + \eta_y^2 + \eta_z^2$$

$$g^{\eta\zeta} = \eta_x\zeta_x + \eta_y\zeta_y + \eta_z\zeta_z$$

$$g^{\zeta\xi} = \zeta_x\xi_x + \zeta_y\xi_y + \zeta_z\xi_z$$

$$g^{\zeta\eta} = \zeta_x\eta_x + \zeta_y\eta_y + \zeta_z\eta_z$$

$$g^{\zeta\zeta} = \zeta_x\zeta_x + \zeta_y\zeta_y + \zeta_z\zeta_z$$

REFERENCES

1. Hah, C., "A Navier-Stokes Analysis of Three-Dimensional Turbulent Flows Inside Turbine Blade Rows at Design and Off-Design Conditions," Journal of Engineering for Gas Turbines and Power, Vol. 106, No. 2, Apr. 1984, pp. 421-429.

2. Dawes, W.N., "A Numerical Analysis of the Three-Dimensional Viscous Flow in a Transonic Compressor Rotor and Comparison with Experiment," ASME Paper 86-GT-16, June 1986.

3. Davis, R.T. and Werle, M.J., "Progress on Interacting Boundary Layer Computations at High Reynolds Number," Numerical and Physical Aspects of Aerodynamic Flows, T. Cebeci, Ed., Springer-Verlag, New York, 1982, pp. 187-210.

4. Vatsa, V. N., Werle, M.J., and Verdon, J.M., "Analysis of Laminar and Turbulent Symmetric Blunt Trailing-Edge Flows," United Technologies Research Center, East Hartford, CT, UTRC-R81-914986-5, Apr. 1981. (Avail. NTIS, AD-A098703).

5. Carter, J.E. and Wornom, S.F., "Solutions for Incompressible Separated Boundary Layers Including Viscous-Inviscid Interaction," Aerodynamic Analyses Requiring Advance Computers, Part 1, NASA SP-347, 1975, pp. 125-150.

6. Kim, J., Kline, S.J., and Johnston, J.P., "Investigation of Separation and Reattachment of a Turbulent Shear Layer: Flow Over a Backward-Facing Step," Stanford University, Mechanical Engineering Department, Report MD-37, 1978.

7. Kwon, O.K. and Pletcher, R.H., "Application of a Viscous-Inviscid Interaction Procedure to Predict Turbulent Separating Flows Over a Rearward-Facing Step," Computation of Internal Flows: Methods and Applications, P.M. Sockol and K.N. Ghia, Eds., ASME, New York, 1984, pp. 73-81.

8. Pouagare, M., Lakshiminarayana, B., and Govindan, T.R., "Computation of Viscous Flows in Turbomachinery Cascades With a Space-Marching Method," Journal of Propulsion and Power, Vol. 2, No. 3, May-June 1986, pp. 266-274.

9. Ghia, K.N. and Sokhey, J.S., "Laminar Incompressible Viscous Flow in Curved Ducts of Rectangular Cross Sections," Journal of Fluids Engineering, Vol. 99, No. 4, Dec. 1977, pp. 640-648.

10. Khalil, I.M. and Weber, W.G., "Modeling of Three-Dimensional Flow in Turning Channels," Journal of Engineering for Gas Turbines and Power, Vol. 106, No. 3, July 1984, pp. 682-691.

11. Rhie, C.M., "Basic Calibration of a Partially-Parabolic Procedure Aimed at Centrifugal Impeller Analysis," AIAA Paper 83-0260, Jan. 1983.

12. Rubin, S.G. and Lin, A., "Marching With the Parabolized Navier-Stokes Equations," Israel Journal of Technology, Vol. 18, No. 1-2, 1980, pp. 21-31.

13. Rubin, S.G., "A Review of Marching Procedures for Parabolized Navier-Stokes Equations," Numerical and Physical Aspects of Aerodynamic Flows, T. Cebeci, Ed., Springer-Verlag, New York, 1982, pp. 171-186.

14. Rubin, S.G. and Reddy, D.R., "Global Solution Procedures for Incompressible Laminar Flow With Strong Pressure Interaction and Separation," Numerical and Physical Aspects of Aerodynamic Flows II, T. Cebeci, Ed., Springer-Verlag, New York, 1983, pp. 79-96.

15. Rubin, S.G. and Reddy, D.R., "Analysis of Global Pressure Relaxation for Flows With Strong Interaction and Separation," Computers and Fluids, Vol. 11, No. 4, 1983, pp. 281-306.

16. Reddy, D.R., "Global Pressure Relaxation Procedure for Laminar and Turbulent Incompressible Flows With Strong Interaction and Separation," Ph.D. Dissertation, University of Cincinnati, 1983.

17. Rubin, S.G. and Reddy, D.R., "Global PNS Solutions for Laminar and Turbulent Flow," 6th Computational Fluid Dynamics Conference, AIAA, New York, 1983, pp. 194-203.

18. Reddy, D.R. and Rubin, S.G., "Subsonic/Transonic, Viscous/Inviscid Relaxation Procedures for Strong Pressure Interactions," AIAA Paper 84-1627, June 1984.

19. Reddy, D.R., Delaney, R.A., and Rubin, S.G., "Reduced Navier-Stokes (RNS) Relaxation Procedure for Internal Flows With Interaction," SAE Paper 851790, Oct. 1985.

20. Rudman, S. and Rubin, S.G., "Hypersonic Flow Over Slender Bodies With Sharp Leading Edges," AIAA Journal, Vol. 6, No. 10, Oct. 1968, pp. 1883-1890.

21. Lin, T.C. and Rubin, S.G., "Viscous Flow Over a Cone at Moderate Incidence, I - Hypersonic Tip Region," Computers and Fluids, Vol. 1, No. 1, Jan. 1973, pp. 37-57.

22. Davis, R.T. and Rubin, S.G., "Non-Navier-Stokes Viscous Flow Computations," Computers and Fluids, Vol. 8, No. 1, Mar. 1980, pp. 101-131.

23. Lin, A. and Rubin, S.G., "Three-Dimensional Supersonic Viscous Flow Over a Cone at Incidence," AIAA Journal, Vol. 20, No. 11, Nov. 1982, pp. 1500-1507.

24. Lubard, S.C. and Helliwell, W.S., "An Implicit Method For Three-Dimensional Viscous Flow With Application to Cones at Angle of Attack," Computers and Fluids, Vol. 3, No. 1, Mar. 1975, pp. 83-101.

25. Vigneron, Y.C., Tannehill, J.C., and Rakich, J.V., "Calculation of Supersonic Viscous Flow Over Delta Wings With Sharp Subsonic Leading Edges," AIAA Paper 78-1137, July 1978. (NASA TM-78500).

26. Katsanis, T., "Calculation of Three-Dimensional Viscous Flow Through Turbomachinery Blade Passages by Parabolic Marching," AIAA Paper 85-1408, July 1985. (NASA TM-86984).

27. Schneider, G.E. and Zedan, M., "A Modified Strongly Implicit Procedure for the Numerical Solution of Field Problems," Numerical Heat Transfer, Vol. 4, No. 1, Jan.-Mar. 1981, pp. 1-19.

28. Anderson, D.A., Tannehill, J.C., and Pletcher, R.H., Computational Fluid Mechanics and Heat Transfer, Hemisphere Publishing Corporation, Washington, D.C., 1984, pp. 551-557.

29. Ramakrishnan, S.V. and Rubin, S.G., "Global Pressure Relaxation for Steady, Compressible, Laminar, 2-Dimensional Flows With Full Pressure Coupling and Shock Waves," University of Cincinnati, Report No. AFL-84-100, July 1984.

30. Rubin, S.G., Khosla, P.K., and Saari, S., "Laminar Flow in Rectangular Channels," Computers and Fluids, Vol. 5, No. 3, Sept. 1977, pp. 151-173.

31. Goldstein, R.J. and Kreid, D.K., "Measurement of Laminar Flow Development in a Square Duct Using Laser-Doppler Flowmeter," Journal of Applied Mechanics, Vol. 34, No. 4, Dec. 1967, pp. 813-818.

32. Kreskovsky, J.P., Briley, W.R., and McDonald, H., "Prediction of Laminar and Turbulent Primary and Secondary Flows in Strongly Curved Ducts," NASA CR-3388, 1981.

33. Mori, Y., Uchida, Y., and Ukon, T., "Forced Convective Heat Transfer in a Curved Channel With a Square Cross Section," International Journal of Heat and Mass Transfer, Vol. 14, No. 11, Nov. 1971, pp. 1787-1805.

LEGEND

ξ	STREAMWISE DISTANCE
ω	PRESSURE GRADIENT SPLITTING PARAMETER
u	VELOCITY
p	PRESSURE
i	INDEX IN STREAMWISE DIRECTION

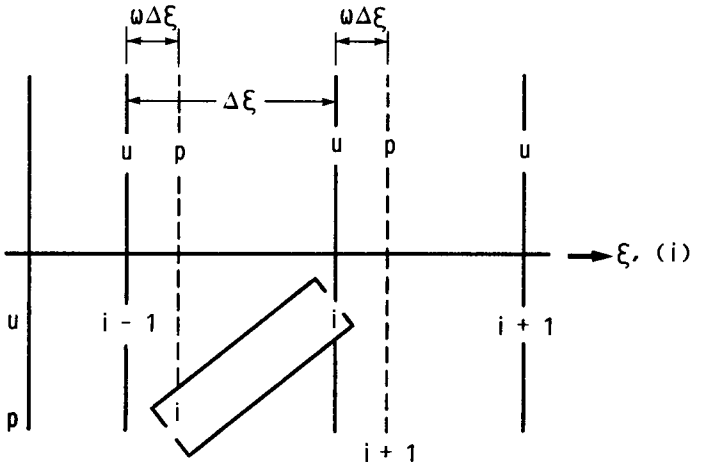

FIGURE 1. - DISCRETIZATION IN THE ξ-DIRECTION.

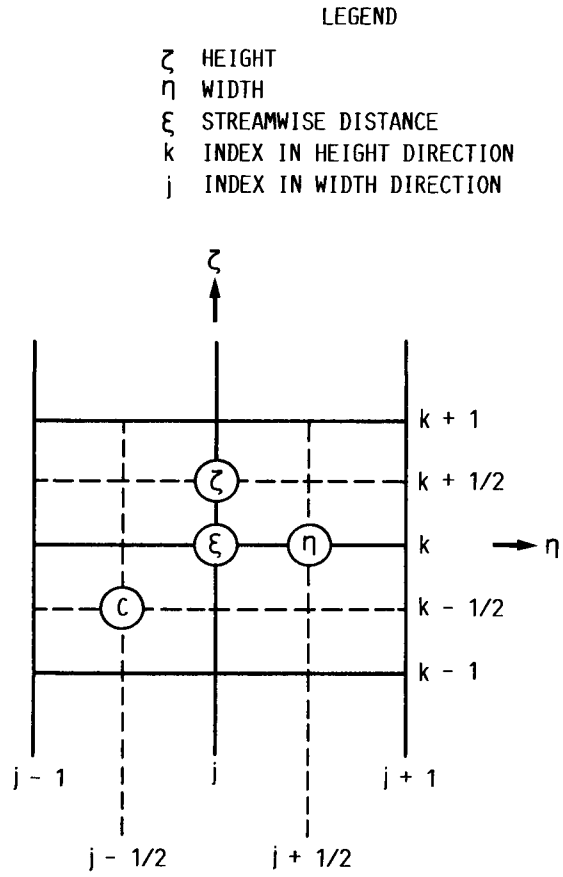

FIGURE 2. - DISCRETIZATION IN THE CROSS-PLANE.

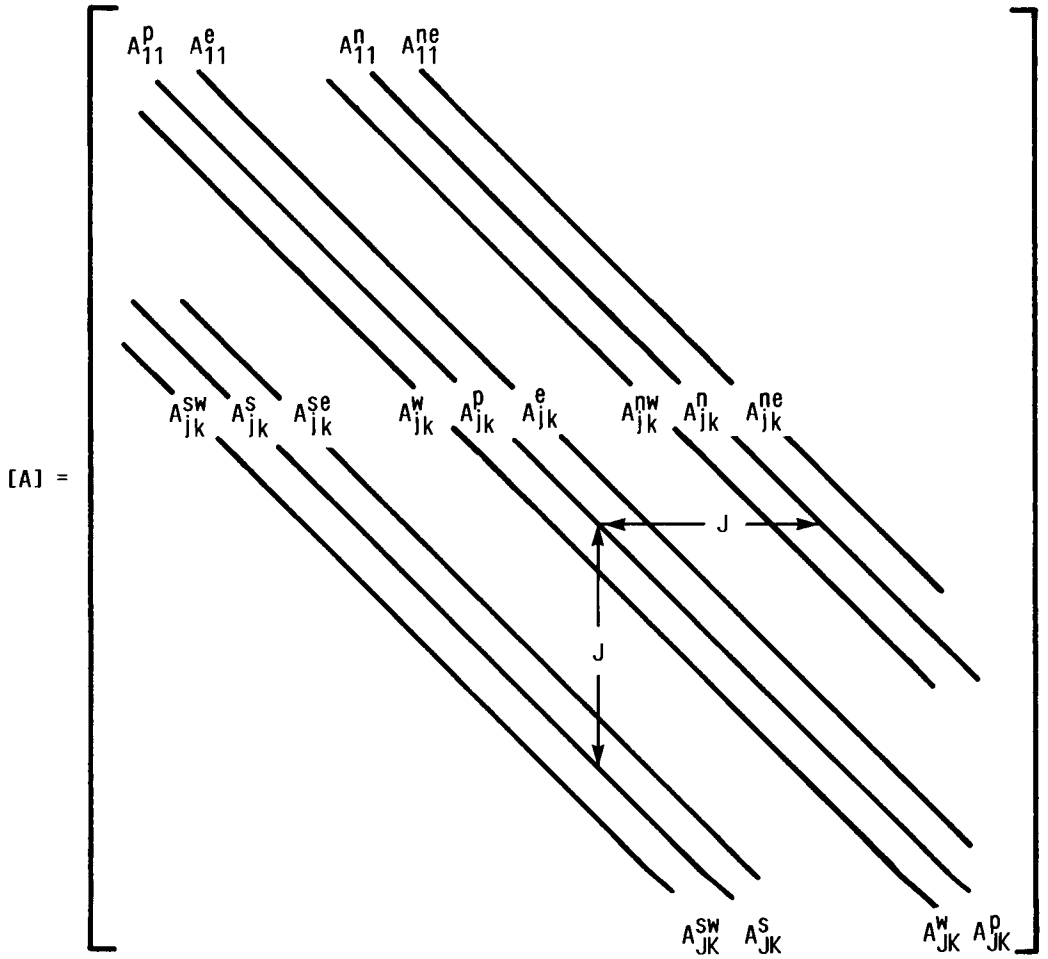

FIGURE 3. - COEFFICIENT MATRIX FOR NINE-POINT FORMULATION.

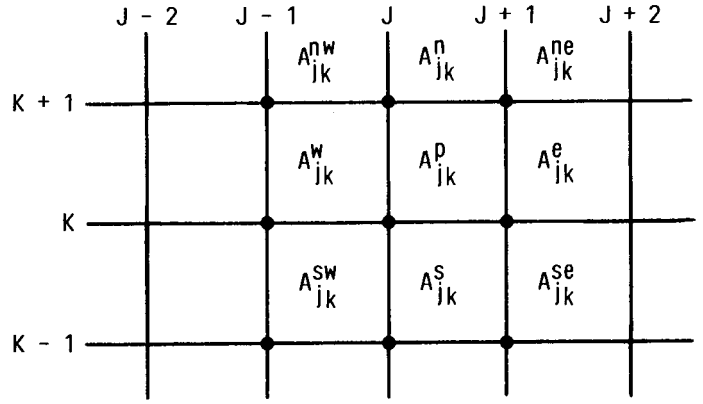

FIGURE 4. - COMPUTATIONAL MOLECULE IN THE CROSS PLANE.

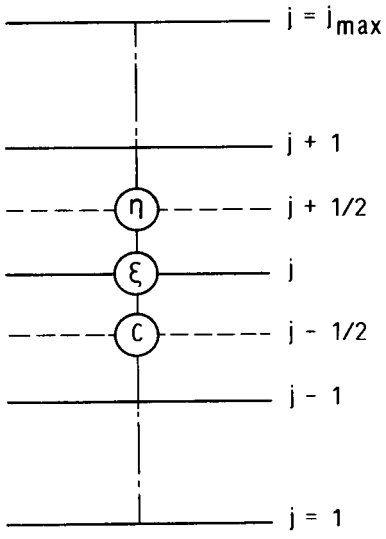

FIGURE 5. - DISCRETIZATION FOR 2-D CASE IN THE NORMAL (η) DIRECTION.

$$
\begin{bmatrix}
\begin{bmatrix} B_{11}B_{12}B_{13} \\ B_{21}B_{22}B_{23} \\ B_{31}B_{32}B_{33} \end{bmatrix}_1 & \begin{bmatrix} C_{11}C_{12}C_{13} \\ C_{21}C_{22}C_{23} \\ C_{31}C_{32}C_{33} \end{bmatrix}_1 & & \\
\begin{bmatrix} A_{11}A_{12}A_{13} \\ A_{21}A_{22}A_{22} \\ A_{31}A_{32}A_{33} \end{bmatrix}_j & \begin{bmatrix} B_{11}B_{12}B_{13} \\ B_{21}B_{22}B_{23} \\ B_{31}B_{32}B_{33} \end{bmatrix}_j & \begin{bmatrix} C_{11}C_{12}C_{13} \\ C_{21}C_{22}C_{23} \\ C_{31}C_{32}C_{33} \end{bmatrix}_j & \\
& \begin{bmatrix} A_{11}A_{12}A_{13} \\ A_{21}A_{22}A_{23} \\ A_{31}A_{32}A_{33} \end{bmatrix}_{j_{max}} & \begin{bmatrix} B_{11}B_{12}B_{13} \\ B_{21}B_{22}B_{23} \\ B_{31}B_{32}B_{33} \end{bmatrix}_{j_{max}}
\end{bmatrix}
\begin{bmatrix} \begin{pmatrix} U \\ V \\ p \end{pmatrix}_1 \\ \begin{pmatrix} U \\ V \\ p \end{pmatrix}_j \\ \begin{pmatrix} U \\ V \\ p \end{pmatrix}_{j_{max}} \end{bmatrix}
=
\begin{bmatrix} \begin{pmatrix} D_1 \\ D_2 \\ D_3 \end{pmatrix}_1 \\ \begin{pmatrix} D_1 \\ D_2 \\ D_3 \end{pmatrix}_j \\ \begin{pmatrix} D_1 \\ D_2 \\ D_3 \end{pmatrix}_{j_{max}} \end{bmatrix}
$$

FIGURE 6. - BLOCK TRIDIAGONAL SYSTEM AT MARCHING LOCATION (i) FOR 2-D FLOW.

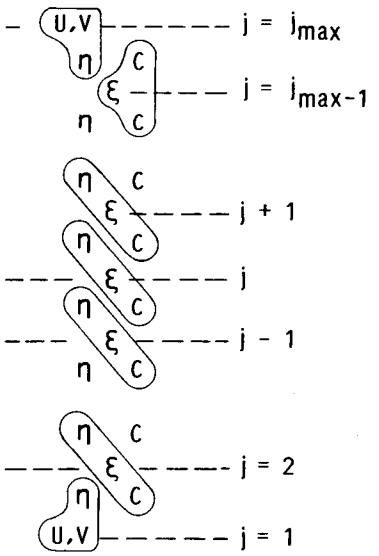

FIGURE 7. - GROUPING OF DISCRETIZATION GOVERNING EQUATIONS IN THE FLOW FIELD.

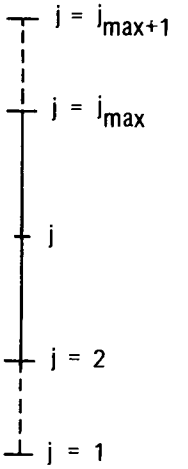

FIGURE 8. - PERIODIC BOUNDARIES FOR 2-D CASE.

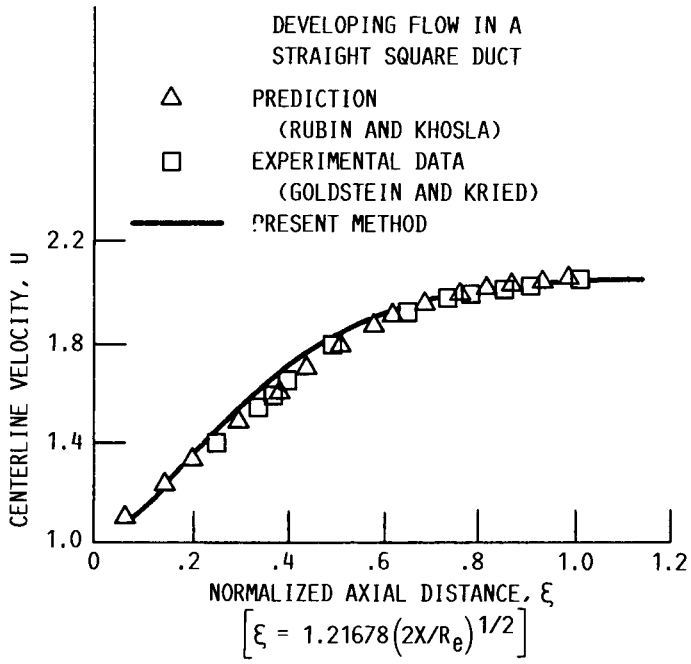

FIGURE 9. - CENTERLINE VELOCITY VARIATION.

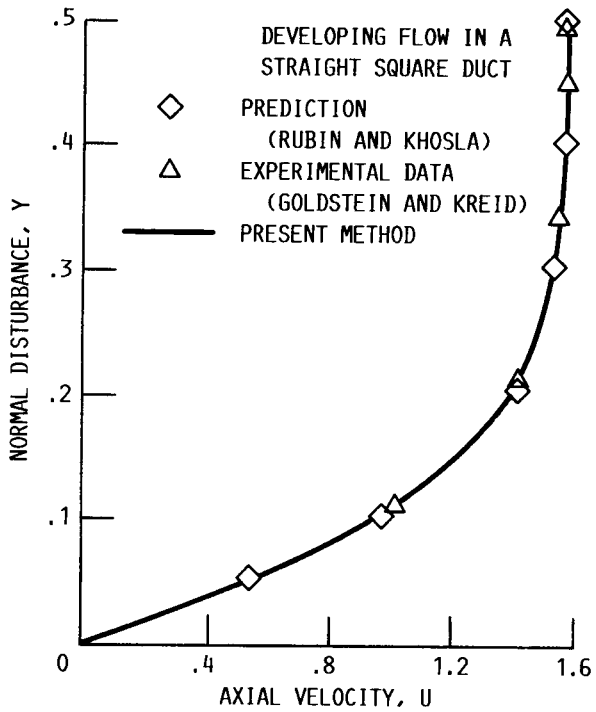

FIGURE 10. - AXIAL VELOCITY PROFILE AT
$\xi = 0.295$, $Z = 0$.

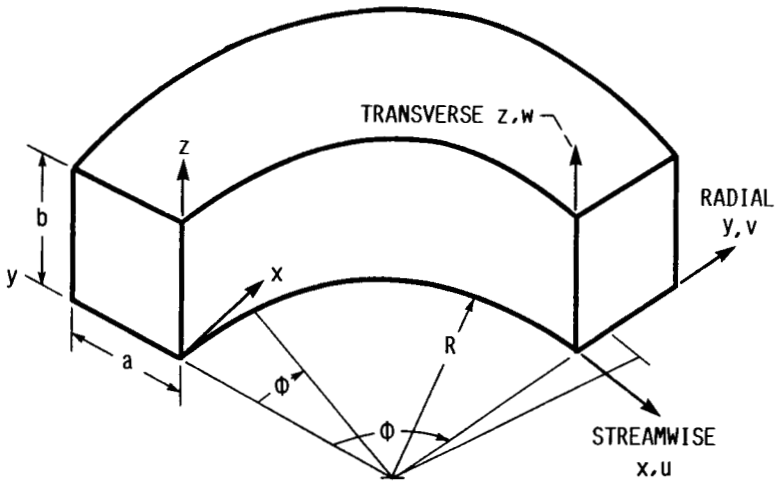

HYDRAULIC DIAMETER H = 2ab/(a + b)

FIGURE 11. - CURVED DUCT GEOMETRY AND COORDINATE SYSTEM.

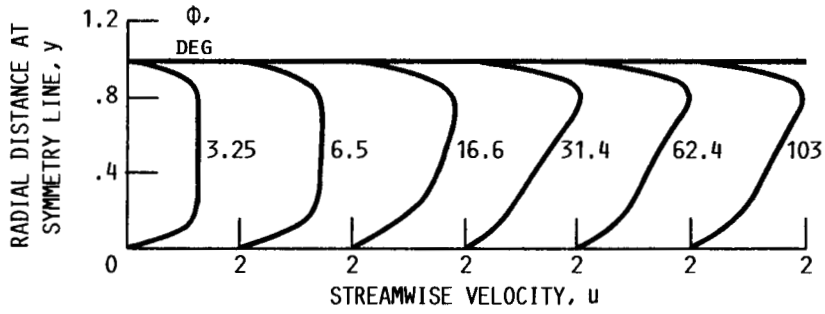

FIGURE 12. - DEVELOPMENT OF PRIMARY VELOCITY PROFILE FOR A CIRCULAR ARC DUCT OF SQUARE CROSS SECTION, Re = 205, R/H = 14, K = 55.

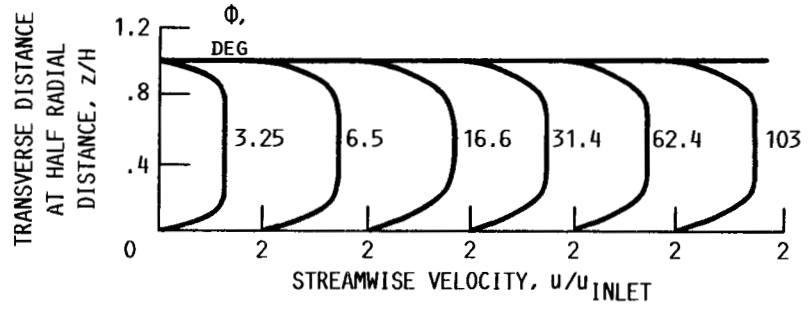

FIGURE 13. - DEVELOPMENT OF PRIMARY VELOCITY PROFILE IN THE TRANSVERSE PLANE FOR A CIRCULAR ARC DUCT OF SQUARE CROSS SECTION, Re = 205, R/H = 14, K = 55.

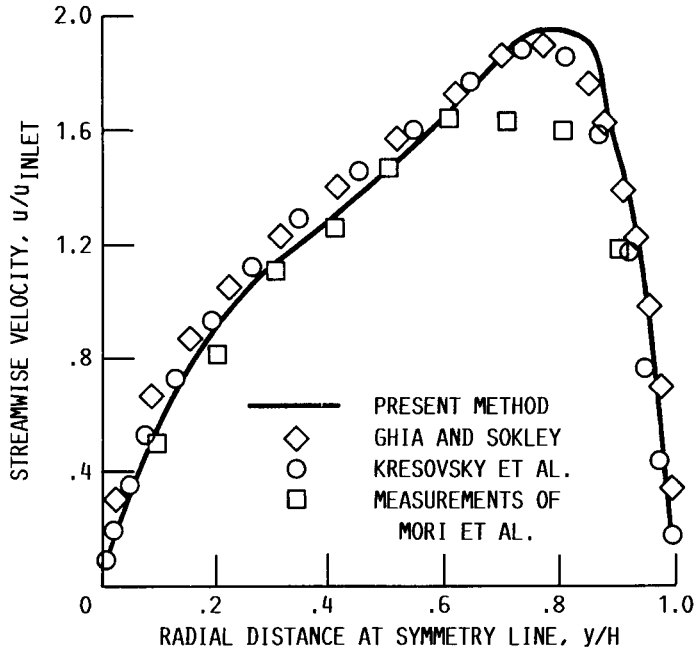

FIGURE 14. - FULLY DEVELOPED PRIMARY FLOW VELOCITY PROFILE FOR A CIRCULAR ARC DUCT OF SQUARE CROSS SECTION, R/H = 14, Re = 205, K = 55.

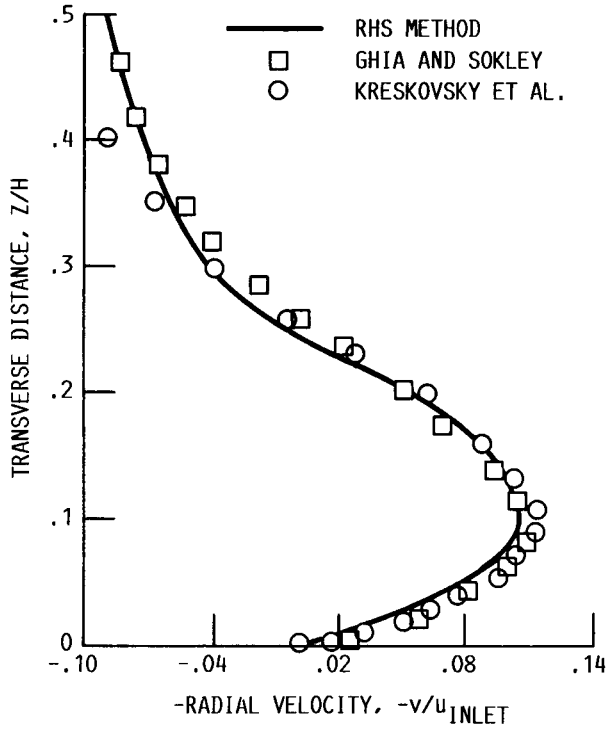

FIGURE 15. - FULLY DEVELOPED RADIAL VELOCITY PROFILE AT y/H = 0.4 FOR A CIRCULAR ARC DUCT OF SQUARE CROSS SECTION, R/H = 14, Re = 205, K = 55.

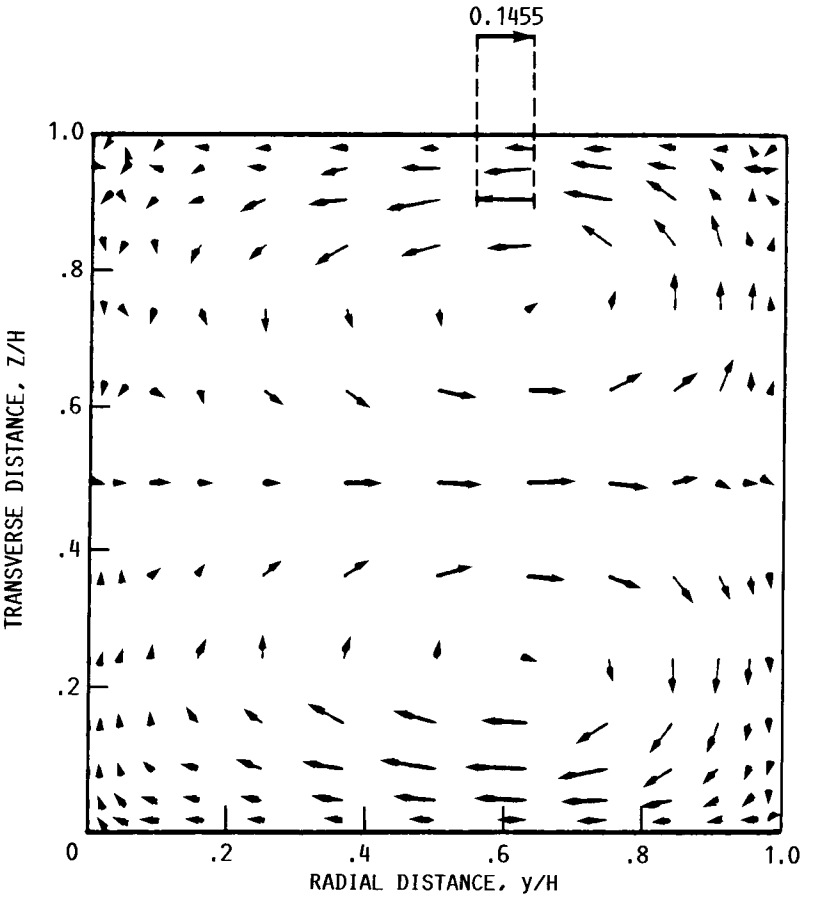

FIGURE 16. - FULLY DEVELOPED SECONDARY FLOW VELOCITY IN A CIRCULAR ARC DUCT, Re = 205, R/H = 14, K = 55.

NASA
National Aeronautics and Space Administration

Report Documentation Page

1. Report No.	2. Government Accession No.	3. Recipient's Catalog No.
NASA CR-180874 AIAA-88-0714		

4. Title and Subtitle

Consistent Boundary Conditions for Reduced Navier-Stokes (RNS) Scheme Applied to Three-Dimensional Internal Viscous Flows

5. Report Date

6. Performing Organization Code

7. Author(s)

D.R. Reddy and S.G. Rubin

8. Performing Organization Report No.

E-3739-1

10. Work Unit No.

505-62-21

9. Performing Organization Name and Address

Sverdrup Technology, Inc.
Lewis Research Center
Cleveland, Ohio 44135-3191

11. Contract or Grant No.

NAS3-24105

13. Type of Report and Period Covered

Contractor Report
Final

12. Sponsoring Agency Name and Address

National Aeronautics and Space Administration
Lewis Research Center
Cleveland, Ohio 44135-3191

14. Sponsoring Agency Code

15. Supplementary Notes

Project Manager, Peter M. Sockol, Internal Fluid Mechanics Division, NASA Lewis Research Center. D.R. Reddy, Sverdrup Technology. Inc.; S.G. Rubin, University of Cincinnati, Ohio 45221, Dept. of Aerospace Eng. and Eng. Mechanics. Prepared for the 26th Aerospace Science Meeting sponsored by the American Institute of Aeronautics and Astronautics, Reno, Nevada, January 11-14, 1988.

16. Abstract

A consistent and efficient set of boundary conditions are developed for the multi-sweep space marching pressure-elliptic Reduced Navier-Stokes (RNS) scheme as applied for three-dimensional internal viscous flow problems. No-slip boundary conditions are directly imposed on the solid walls. There is no iteration procedure required in the cross plane to ensure mass conservation across each marching plane. The finite difference equations forming the coefficeint matrix are ordered such that the surface normal velocity is specified on all the solid walls; unlike external flows, a pressure boundary conditions in the cross plane is not required. Since continuity is directly satisfied at all points in the flow domain, the first order momentum equations can be solved directly for the pressure without the need for a Poisson pressure correction equation. The procedure developed herein can also be applied with periodic boundary conditions. The analysis is given for general compressible flows. Incompressible flow solutions are obtained, for straight and curved ducts of square cross section, to validate the procedure. The solutions of these test cases are used to demonstrate the applicability of the RNS scheme, with the improved boundary conditions for internal flows with strong interaction, as would be encountered in ducts and turbomachinery geometries.

17. Key Words (Suggested by Author(s))	18. Distribution Statement
Computational fluid dynamics; Reduced Navier-Stokes Scheme; Three-dimensional viscous/inviscid interaction	Unclassified - Unlimited Subject Category 02

19. Security Classif. (of this report)	20. Security Classif. (of this page)	21. No of pages	22. Price*
Unclassified	Unclassified	18	A02

*For sale by the National Technical Information Service, Springfield, Virginia 22161